

## Research Article

# Poly- $\gamma$ -Glutamic Acid Nanoparticles Based Visible Light-Curable Hydrogel for Biomedical Application

József Bakó,<sup>1</sup> Farkas Kerényi,<sup>1</sup> Edit Hrubí,<sup>1</sup> István Varga,<sup>2</sup> Lajos Daróczi,<sup>3</sup> Beatrix Dienes,<sup>4</sup> László Csernoch,<sup>4</sup> József Gáll,<sup>5</sup> and Csaba Hegedűs<sup>1</sup>

<sup>1</sup>Department of Biomaterials and Prosthetic Dentistry, University of Debrecen, Nagyerdei krt. 98, Debrecen 4032, Hungary

<sup>2</sup>Department of Periodontology, University of Debrecen, Nagyerdei krt. 98, Debrecen 4032, Hungary

<sup>3</sup>Department of Solid State Physics, University of Debrecen, Nagyerdei krt. 98, Debrecen 4032, Hungary

<sup>4</sup>Department of Physiology, University of Debrecen, Nagyerdei krt. 98, Debrecen 4032, Hungary

<sup>5</sup>Department of Applied Mathematics and Probability Theory, University of Debrecen, Nagyerdei krt. 98, Debrecen 4032, Hungary

Correspondence should be addressed to Csaba Hegedűs; [hegedus.csaba.prof@dental.unideb.hu](mailto:hegedus.csaba.prof@dental.unideb.hu)

Received 18 January 2016; Accepted 12 May 2016

Academic Editor: Ester Vazquez

Copyright © 2016 József Bakó et al. This is an open access article distributed under the Creative Commons Attribution License, which permits unrestricted use, distribution, and reproduction in any medium, provided the original work is properly cited.

Nanoparticles and hydrogels have gained notable attention as promising potential for fabrication of scaffolds and delivering materials. Visible light-curable systems can allow for the possibility of *in situ* fabrication and have the advantage of optimal applicability. In this study nanogel was created from methacrylated poly- $\gamma$ -glutamic acid nanoparticles by visible (dental blue) light photopolymerization. The average size of the particles was 80 nm by DLS, and the NMR spectra showed that the methacrylation rate was 10%. Polymerization time was 3 minutes, and a stable nanogel with a swelling rate of 110% was formed. The mechanical parameters of the prepared structure (compression stress 0.73 MPa, and Young's modulus 0.93 MPa) can be as strong as necessary in a real situation, for example, in the mouth. A retaining effect of the nanogel was found for ampicillin, and the biocompatibility of this system was tested by Alamar Blue proliferation assay, while the cell morphology was examined by fluorescence and laser scanning confocal microscopy. In conclusion, the nanogel can be used for drug delivery, or it can be suitable for a control factor in different systems.

## 1. Introduction

Nanotechnology is one of the most promising possibilities to reach various special aims, in the field of biomedical devices and particularly in drug delivery. Nanoparticle-based systems have received increasing interest because the high surface to volume ratio ensures well-tailorable physical and chemical properties [1]. The application of synthetic or biodegradable polymer nanoparticles has been widely investigated in sensor technology, forensic science, or medical therapy [2–5]. This group of 1–100 or sometimes 1–1000 nm particles can carry drugs that are dissolved, entrapped, encapsulated, or attached to the particles. In these ways nanoparticles, nanospheres, or nanocapsules were created [6–10].

Under appropriate circumstances, many of these polymers form hydrogels and can improve the bioavailability of

low or high molecular weight drugs or other biologically active agents [11–14]. Hydrogels resemble natural tissues and due to their high water content they can deliver these materials in a minimally invasive manner [15–17]. These nanoparticle/active-agent formulations reduce the risk of toxicity and side effects, and they increase efficiency, specificity, and tolerability, which are the therapeutic index of drugs [18–20].

Poly- $\gamma$ -glutamic acid ( $\gamma$ -PGA) is a polyamino acid formed by the amide bond linkage between the amino group on the  $\alpha$ -carbon and the carboxyl group on the  $\gamma$ -carbon.  $\gamma$ -PGA is a naturally occurring anionic homopolyamide that is biodegradable, edible, nontoxic, and nonimmunogenic [21]. This polymer is well known and has been investigated for many special aims; for example, it is a good candidate for biomedical applications, tissue engineering, or drug delivery

systems [22–24]. Different copolymer forms and hydrogels were created to realize the wide range of possibilities [25]. In the near past, nanoparticles were created from this material, and they were used for antigen protein encapsulation and for manipulating the antigen-specific immune response [26–28].

Visible light photopolymerization has been widely used in the field of dentistry. This polymerization is not as widespread generally as the other (higher energy used) methods. The lower energy cannot cause any harmful effects, and this advantage is important in biomaterials. In our previous study a  $\gamma$ -PGA-based photopolymerizable hydrogel was developed, and it was described as an alternative drug delivery vehicle [29]. Recognizing the new possibilities of nanoparticles we enhanced the original concept.

The aim of this study was to prepare and to characterize a light cured methacrylated  $\gamma$ -PGA nanoparticle-created hydrogel system (PGA nanogel) which can be used practically *in situ*. To achieve the objective, the reactive NP synthesis and fast nanogel creation were demonstrated. The mechanical properties, swelling kinetics, and release profile of ampicillin were investigated, and finally, Alamar Blue assay was performed to assess the biocompatibility of the nanogel system; the proliferation behavior of the cells was demonstrated by fluorescence and confocal laser scanning microscopy.

## 2. Material and Methods

**2.1. Modifications of PGA.** The poly- $\gamma$ -glutamic acid ( $\gamma$ -PGA,  $M_w = 1.2 \times 10^6$ , from GPC) was purchased from Nanjing Saitaisi Biotechnology Co. Ltd. (Nanjing, China); in the first step, nanoparticles (NPs) were created as previously described [30]. Water-soluble 1-[3-(dimethylamino) propyl]-3-ethylcarbodiimide hydrochloride (EDC) (Carbosynth Limited, Compton, Berkshire, UK), 2,2'-(ethylenedioxy)bis(ethylamine) (98%) (EDA) as crosslinker, 2-aminoethyl methacrylate hydrochloride (90%) (AEM) as methacrylating agent, and ampicillin sodium salt as active substance were purchased from Sigma Aldrich (St. Louis, MO, USA). Irgacure 2959 (~99%, CIBA) was applied as photoinitiator. In the first step, the biocompatible and biodegradable  $\gamma$ -PGA was activated by EDC, and EDA was used for creation of PGA-NPs. In the next step, the remaining carboxyl groups were activated by EDC, and the created PGA-NPs were modified by methacryloyl group used by AEM. The polymer concentration was 10 mg/mL in water, and the reaction time was 24 hours per step. The purification of methacrylated-PGA-NPs was done with Vivaflow 200 (MWCO 10.000 Da, PES) used by minimum fivefold amount of water. The purified polymer was freeze-dried in a Virtis Freeze Drier (CHRIST ALPHA 1-2) under vacuum at  $-52^\circ\text{C}$  for 4 days. The scheme for chemical modifications of PGA is demonstrated in Figure 1. These methacrylated poly- $\gamma$ -glutamic acid nanoparticles (MPGA-NPs) can be polymerized using visible (blue) light, which can be found in the dental practice.

**2.2. Characterization of the Methacrylated Nanoparticles (MPGA-NPs).** Molecular characterization of the modified PGAs (MPGA-NPs) was accomplished by Proton Nuclear

Magnetic Resonance Spectroscopy ( $^1\text{H}$  NMR) on a Bruker 200SY NMR spectrometer (200 MHz) instrument. Samples were dissolved in deuterated water ( $\text{D}_2\text{O}$ ) and the chemical shifts were represented in parts per million (ppm) based on the signal of sodium 3-(trimethylsilyl)-propionate- $\text{d}_4$  as a reference.

Dynamic light scattering measurement was performed for the determination of the hydrodynamic diameter (HD) of the NPs using a goniometer equipped with a NdYAG solid state laser (BI-200SM Brookhaven Research Laser Light Scattering, Brookhaven Instruments Co., USA); the operating wavelength was  $\lambda_0 = 532\text{ nm}$ . Measurements of the average size of the NPs were performed at  $25^\circ\text{C}$  with an angle detection of  $90^\circ$  in optically homogeneous quartz cylinder cuvettes. The samples were prepared from freeze-dried material. The concentration of the polymer dispersion was 0.5 mg/mL.

**2.3. Synthesis of PGA Nanogel.** MPGA-NPs based hydrogels (PGA nanogel) were synthesized by free radical-initiated photopolymerization in saline solution. 33 w/w% of MPGA-NPs were mixed with the solution of the photoinitiator (2 n/n% for methacryloyl group). The photopolymerization took place in a Dentacolor XS (Kulzer, Germany) photopolymerization chamber (435 nm,  $\sim 3\text{ watt/cm}^2$ ). The reaction time was 180 s in flash mode. The molds of the samples were cylindrical, with a depth of 2 mm and a diameter of 5 mm, and were made of Teflon.

**2.4. Characterization of the PGA Nanogel.** The PGA nanogels were dehydrated with acetone/water solutions and were dried at critical point using  $\text{CO}_2$ ; finally, they were sputter-coated with gold for 30 s. The plasma current was 18–20 mA, while the sputtering Ar pressure was 10–20 mPa during the coating. The thickness of the deposited Au layer was about 100 nm. Samples were imaged using a scanning electron microscope (SEM, Hitachi S4300 CFE, Tokyo, Japan) at an accelerating voltage of 10 kV.

The mechanical properties of the PGA nanogels were investigated with an INSTRON 5544 Universal Mechanical Analyzer (Instron, USA). The compression tests were performed on cylindrical samples with full scale load range at 0.1 kN and crosshead speed at 2 mm/min. The cylindrical hydrogel samples had a diameter of 5 mm and specimen length of 2 mm.

Gravimetric analysis of the PGA nanogel was performed for the swelling experiments. It was carried out by immersion of nanogels in saline solution. At predefined intervals of time, the samples were removed from water and wiped with bolting paper to eliminate the excess water. The measurements were iterated until the hydrated gels achieved a constant weight value. The weight swelling percentage (Wp) for each sample was calculated as follows:

$$W_p = \frac{(W_s - W_o)}{W_o} \times 100, \quad (1)$$

where  $W_s$  is the weight of the swollen gel and  $W_o$  is the original weight of the gel after polymerization.

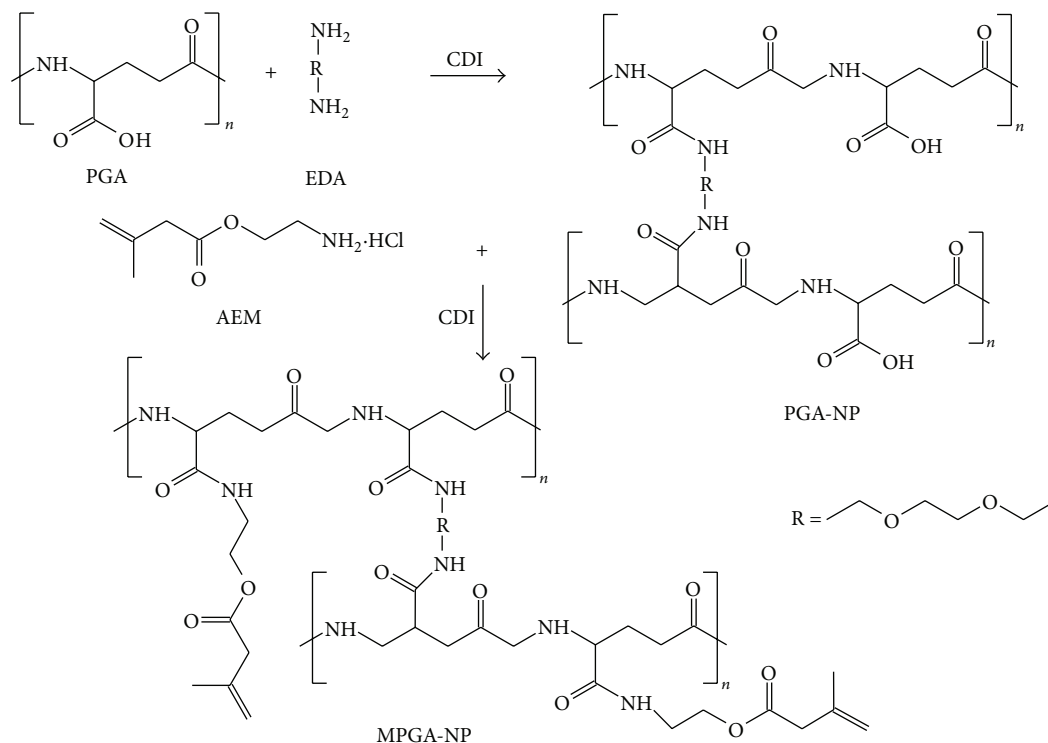


FIGURE 1: Scheme of the chemical reaction for the modifications of  $\gamma$ -PGA. The first step is a crosslinking reaction, where the CDI activates the carboxyl groups and the EDA creates crosslinked  $\gamma$ -PGAs. 24 hours later, in the second step a methacrylation reaction takes place, where the remaining carboxyl groups will be activated by a new portion of CDI and the AEM will form methacrylated-PGA nanoparticles (MPGA-NPs).

The PGA nanogels were prepared for release studies with 3.33 mg/g ampicillin content. The main purpose of these experiments was to examine the release rate of the drug from the loaded matrix. The investigated samples were immersed in saline solution (20 mL) and subjected to continuous magnetic stirring. At regular time intervals, an aliquot of 0.2 mL was removed, and the concentration of ampicillin was measured by HPLC; a Dionex Ultimate 3000 (Dionex Softron GmbH, Germering, Germany) instrument was used with Accucore™ aQ (C18, 2.6  $\mu\text{m}$ ) column and UV detection at 210 nm. The mobile phase was 60% saline solution and 40% acetonitrile, and the flow rate was 0.4 mL/min. The removed liquid was replaced by fresh saline solution. The final result was expressed by the percentage of the original drug content. In the cases of mechanical analysis and determinations of swelling and release properties the results of PGA nanogels were compared with methacrylated-PGA hydrogels (MPGA hydrogels) [29]. The schematic illustration of the hydrogel and nanogel creation is shown in Figure 2.

**2.5. Cell Viability Investigation.** Human osteosarcoma-derived SAOS-2 cell line (ATCC, USA) was used for Alamar Blue (Invitrogen, DAL1100) cell proliferation assay.  $9 \times 10^4$  cells/well were placed in a 24-well cell culture plate and cells were let to attach to the bottom of the wells for 4 hours. Attached cells were washed with colorless DMEM (Sigma Aldrich, D5921) and were incubated at 37°C in a  $\text{CO}_2$  incubator for 2 hours in Alamar Blue reagent diluted

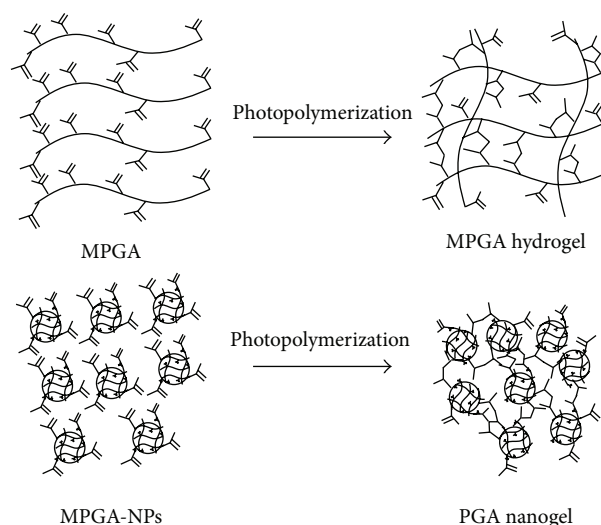


FIGURE 2: Schematic illustration of the creation of the earlier described MPGA hydrogel [29], and the PGA nanogel.

10x in colorless DMEM. The fluorescence of the reduced Alamar Blue was measured by Hidex Sense Microplate Reader (Hidex Oy, Turku, Finland) using 530 nm light for excitation. The emitted fluorescent light was detected using a 590 nm emission filter and mean fluorescence intensity was determined (indicated on the graph as day 0). After

the measurement, Alamar Blue reagent was replaced with DMEM medium (Sigma Aldrich D6046), in which PGA nanogels (2 mm  $\times$  5 mm gels were used) were submerged using Millipore 24 Well Millicell hanging cell culture inserts 0.4  $\mu$ m PET (Millipore Co. Billerica, MA). Measurements were repeated after 4, 24, 48, and 72 hours. Nanogels were removed every time before the measurements; after the removal of Alamar Blue, the gels were placed back into the wells; therefore the same cells could be measured during the experiment. Nontreated SAOS-2 cells, grown in 2D culture, were used as control. Error bars on the graphs represent the standard deviation (SD) of three parallel measurements.

The effect of the antibiotic ampicillin in free form and loaded into nanogel was compared with a microbiological method. *E. coli* ER2738 (NEB) was seeded in top agar on LB plates. The PGA nanogels with or without ampicillin were placed immediately into the top agar. Ampicillin or saline (as negative control) solution was pipetted in small wells in the top agar. Four parallel plates were used. The ampicillin solution and the loaded PGA nanogels contained the same amounts of antibiotic in each plate. Pictures were taken after 4, 6, 8, and 20 hours with a Canon EOS 70D digital camera. The areas of the plaques were measured using ImageJ software.

**2.6. Cell Imaging Techniques.** The PGA nanogel samples for the different microscopy analyses were fixed chemically to the glass surface. 13 mm diameter #1.5 circle coverslips (Thermo Scientific Menzel GmbH, Germany) were treated with a 1:1 solution of 48 v/v% hydrofluoric acid (VWR International, ECR) and distilled water for 1 min, and after cleaning (twice in distilled water and once in acetone), they were modified with silane molecule (Ultradent® Silane, Ultradent Products Inc., USA). After air-drying, the PGA nanogel was applied as a thin film layer and was chemically attached by 90 s of photopolymerization in a Dentacolor XS chamber. These samples were placed into a 24-well plate and were disinfected for 30 minutes by UV light. Untreated coverslips were used as negative control.

SAOS-2 cells were stained with CellTracker Green BOD-IPY (Molecular Probes, USA) for 30 minutes and then seeded ( $10^5$  cells/well) on coverslips for fluorescence microscopy. Each sample was restained with CellTracker Green for 30 minutes before 24-, 48-, 72-, and 168-hour microscopy. The culture medium was changed and propidium iodide was added before each microscopic examination. Pictures were taken after 6, 24, 48, 72, and 168 hours with Zeiss AxioVert A1 inverted fluorescence microscope (Zeiss, Germany).

SAOS-2 cells were seeded ( $10^5$  cells/well) on coverslips for confocal laser scanning microscopy. Samples were labelled after 6, 24, 48, 72, and 168 hours. An earlier described labelling protocol was modified [31]. Shortly, samples were washed three times in glucose-HEPES buffer (20 mM HEPES, 123 mM NaCl, 5 mM KCl, 1.5 mM  $MgCl_2$ , and 1 mM  $CaCl_2$ ), which was followed by fixation in 1% paraformaldehyde for 10 minutes; then the samples were washed again three times in glucose-HEPES buffer. After A488-phalloidin and Hoechst (Life Technologies, USA) labelling in 0.1% Triton X-100

(Sigma, USA) for 30 minutes, the samples were washed again three times in glucose-HEPES buffer; then they were fixed in 1% paraformaldehyde, covered with Fluorescent Mounting Medium (DAKO, Denmark), and mounted to microscope slides. Confocal images were taken with Zeiss LSM 510 META confocal laser scanning microscope (Zeiss, Germany).

**2.7. Statistical Analysis.** To compare the distributions and the means of the groups, we applied the independent sample *t*-test or Welch's *t*-test depending on the equality of the variances. For the latter question, Levene's *F* test was applied. However, because of the small sample sizes and the possible lack of normality of the original distributions, we also ran the Mann-Whitney test, which can be considered as a nonparametric alternative to the *t*-tests. We also used ANOVA to see the influence of the factors. We used IBM SPSS Statistics 22 for the statistical calculations.

Short list of abbreviations of investigated materials is as follows:

$\gamma$ -PGA: poly-gamma-glutamic acid.

NPs: nanoparticles.

PGA-NPs: poly-gamma-glutamic acid nanoparticles (in our case intermediate).

MPGA-NPs: methacrylated-poly- $\gamma$ -glutamic acid nanoparticles.

PGA nanogel: methacrylated  $\gamma$ -PGA nanoparticle-created hydrogel/nanogel system.

MPGA: methacrylated-PGA polymer.

MPGA hydrogel: methacrylated-PGA hydrogel (based on MPGA polymer, as previously described [29]).

### 3. Results and Discussion

**3.1. Nanoparticle Characterization.** The structure of  $\gamma$ -PGA and MPGA-NP was characterized by NMR spectroscopy. On the basis of the NMR results, the signals of crosslinker can be found on the spectra of MPGA-NP, and the methacryloyl groups were attached to the polymer backbone. The signal assignments were performed as follows  $\delta$  = 4.2 ppm ( $\alpha$ -CH) (Figure 3, PGA molecule). Further signals were determined from the PGA backbone  $\delta$  = 2.4 ppm ( $\gamma$ -CH<sub>2</sub>) and  $\delta$  = 2.09 and 1.95 ppm ( $\beta$  and  $\beta'$ -CH<sub>2</sub>) and  $\delta$  = 3.23, 3.62, 3.70 ppm ( $-\text{CH}_2$  groups) for the crosslinker moiety from EDA. The signals of the methacryloyl group were assigned  $\delta$  = 6.09, 5.70, and 1.88 ppm. These peaks show that the initial crosslinking and the subsequent methacrylating reactions were successful; the signals of different groups could be found in the spectrum. The intensities of the methacryloyl peaks are lower (10%) than the calculated value (50%), but this reactive group allowed the fast photocrosslinking reaction. This phenomenon is not unknown; Zeng et al. reported similar results in connection with a comparable system [23].

Particle sizes of the created MPGA-NPs were determined by DLS measurements. The measured sizes of NPs ranged from a few dozen (20–40) to a few hundred (100–200) nanometers (Figure 4). The average diameter was around



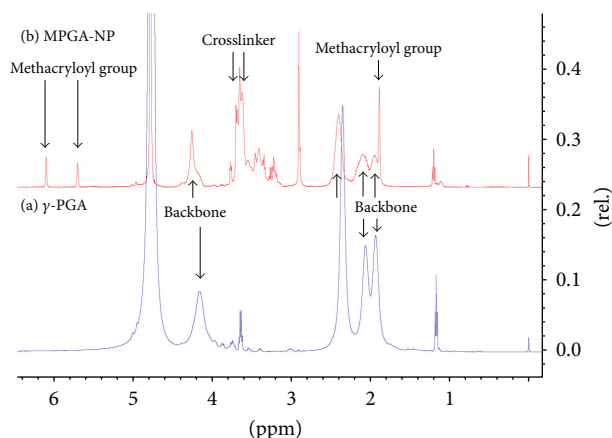


FIGURE 3:  $^1\text{H}$  NMR spectra of (a)  $\gamma$ -PGA and (b) MPGA-NP. Note: the chemical shift values of the methacryloyl groups are  $\delta = 6.09$ ,  $5.70$ , and  $1.88$  and  $\delta = 3.23$ ,  $3.62$ , and  $3.70$  ( $-\text{CH}_2$ ) for the crosslinker. The base material chemical shifts are  $\delta = 4.2$  ppm ( $\alpha$ -CH),  $\delta = 2.4$  ppm ( $\gamma$ - $\text{CH}_2$ ), and  $\delta = 2.09$  and  $1.95$  ppm ( $\beta$  and  $\beta'$ - $\text{CH}_2$ ).

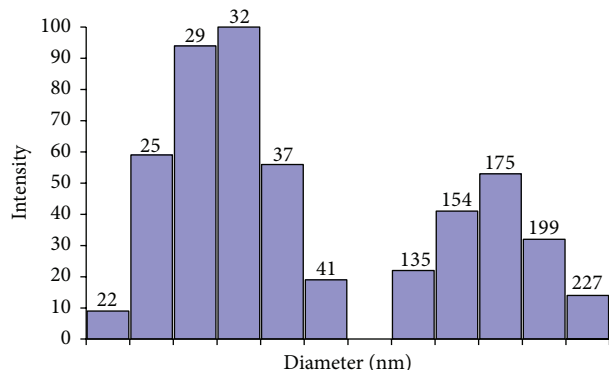


FIGURE 4: DLS particle size distribution profiles of the nanoparticles.

80 nm in the different measurements. The volume distribution shows bimodal characteristic, but the ratios of these two groups show that the vast majority of the NPs are represented in the smaller size (22–41 nm) group (Table 1). The distributions by intensity values show other results. In this case however, the overrepresentation of the larger particles is due to the calculation formula used. However all of the results proved that the particles were nanosized.

### 3.2. Description of the PGA Nanogel

**3.2.1. Demonstration of Nanogel Structure.** The SEM micrographs confirmed the DLS results, because the different nanoscale morphology was clearly visible on the surface images in the deeper regions of the hydrogels and also on the broken surface (Figure 5). Figure 5(a) shows the superficial surface of the PGA nanogel. In the image small particles can be recognized. The nanogel consists of these less than 200 nm sized particles. Image of the broken surface can be seen in Figure 5(b). Different reticulate structures could be found in the nanogels; these structures also had nanoscale dimensions.

TABLE 1: Size distribution of MPGA-NPs according to the DLS result (lower means 22–41 nm and upper 135–227 nm fraction of the polymer).

| Distribution (%) | MPGA-NP |       |
|------------------|---------|-------|
|                  | Lower   | Upper |
| By intensity     | 37      | 63    |
| By volume        | 94      | 6     |
| By number        | 100     | 0     |

TABLE 2: Mechanical parameters of MPGA hydrogels and PGA nanogels.

|               | Compressive strain at break (mm/mm) | Compressive stress at break (MPa) | Young's modulus (MPa) |
|---------------|-------------------------------------|-----------------------------------|-----------------------|
| MPGA hydrogel | $0.452 \pm 0.086$                   | $1.484 \pm 0.503$                 | $4.321 \pm 1.364$     |
| PGA nanogel   | $0.529 \pm 0.124$                   | $0.730 \pm 0.363$                 | $0.926 \pm 0.433$     |

The dimensions of the filaments and particles ranged from 50 to 100 nm.

**3.2.2. Mechanical Parameters, Swelling, and Release Properties of the Nanogel.** Relatively short, 3 minutes, photopolymerization time is enough to obtain a flexible and stable gel. The mechanical stability of the prepared structure can be as strong and as stable as necessary for an application in a real situation, for example, in the mouth [32–34]. Mechanical testing shows that the couplings of the methacrylated nanoparticles are not as complete as in the case of MPGA hydrogel. Despite this, the results showed that, in this way, dimensionally stable structure can be formed from MPGA-NPs. The results of the compression tests showed that the strain of the PGA nanogels can achieve higher values. The differences are in the modulus and in the stress parameters; the MPGA hydrogel reaches considerably higher values, in the case of stress (1.48 MPa), which is double the value of the nanogel (0.73 MPa) (Table 2). Young's modulus shows an even more explicit, MPGA hydrogel (4.32 MPa) and PGA nanogel (0.93 MPa), more than fourfold, difference. The statistical analysis clearly shows that the means (and the distributions) of Young's Modulus values of the two cases, MPGA hydrogels and PGA nanogels, differ significantly (Table 3). Nevertheless the most important fact is that these mechanical parameters of the reactive nanoparticle-created hydrogel could be suitable for application. Its mechanical properties ensure that the PGA nanogel can maintain its 3D structure and could be useable for dental applications (e.g., next to a tooth in a pocket that is only covered by gum) [35, 36]. The mechanical properties of this gel are comparable with or better than other PGA-created hydrogels [23, 37]. The photograph of the prepared gels (Figure 6) also shows noticeable sharp edges and well-defined shapes as evidence for the successful photopolymerization reaction at a depth of 2 mm.

The swelling properties of the gels are definitely related to the structure (Figure 7). This explains why a 125% liquid

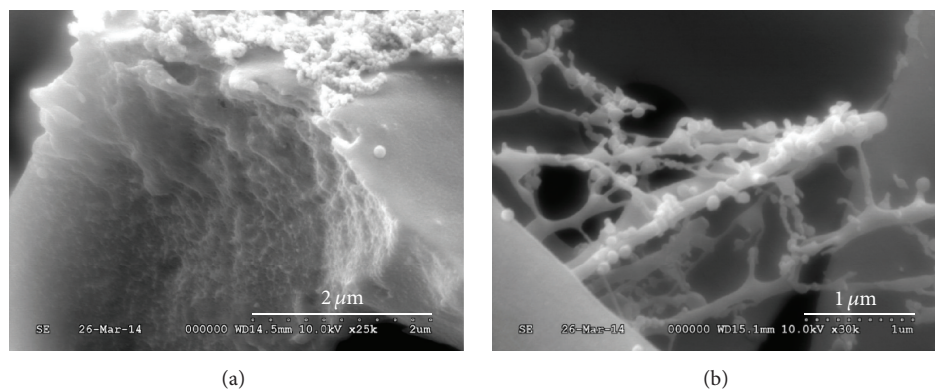


FIGURE 5: SEM images of superficial (a) and broken surfaces (b) of the PGA nanogel. Notes: image (a) was obtained at lower magnification: 25 k ( $\times 25000$ ); image (b) was obtained at higher magnification: 30 k ( $\times 30000$ ).

TABLE 3: Statistical analysis of Young's modulus values of hydrogels.

| Group         | <i>N</i> | Mean  | Std. error of mean | Std. deviation | Levene's <i>F</i> test statistic ( <i>P</i> value) | Welch's <i>t</i> -test statistic (df, <i>P</i> value) | Mann-Whitney test statistic ( <i>P</i> value) |
|---------------|----------|-------|--------------------|----------------|--|---|---|
| MPGA hydrogel | 10       | 4.321 | 0.431              | 1.364          | 7.252  | 7.500   | −3.704  |
| PGA nanogel   | 10       | 0.927 | 0.137              | 0.433          | (0.015)  | (df = 10.792, <i>P</i> value < $10^{-4}$ )            | ( <i>P</i> value < $10^{-3}$ )                |



FIGURE 6: Prepared methacrylated-PGA nanoparticle-created hydrogels (PGA nanogels).

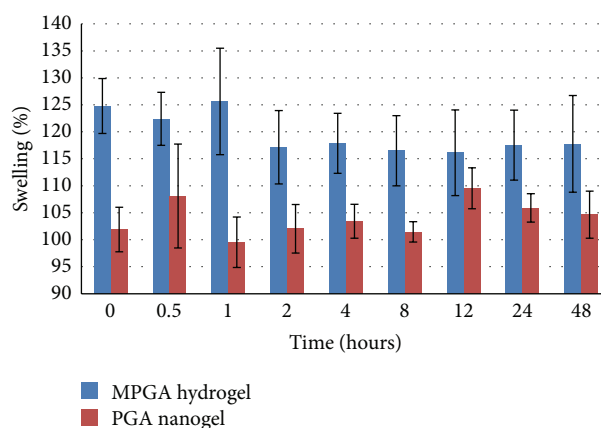


FIGURE 7: The swelling properties of MPGA hydrogels and PGA nanogels.

uptake was found in the case of the MPGA hydrogel and only 110% in the PGA nanogel. The more compact structures of the particle-based system could cause this difference, which is an advantageous parameter considering the fact that the possibility of swelling in the field of the applications is limited (e.g., next to a tooth in a pocket, a greater volumetric change would not be desirable). The first kinetic stage of the swelling is relatively fast and reaches the equilibrium state in the first hour.

The release properties of the PGA nanogel were studied with the generally used antibiotic drug ampicillin. The kinetics of release show initial burst release that reaches the maximum in the 4th hour, and after that the MPGA hydrogel and the PGA nanogel achieve steady state within 24 hours. This status does not change in the remaining days (Figure 8). In similar conditions the free drug solution would become

diluted in the first few seconds or minutes, but the polymer matrix delays this process. The main difference between the hydrogels is that the nanoparticle-based system, the PGA nanogel, demonstrates a retentive effect and can give us a possibility for control. This remaining part of the drug could be mobilized due to the biodegradability of the PGA as a natural process in the circumstances of application. These *in vitro* results were obtained from 20 mL of saline solution and ~40 mg hydrogel/nanogel samples. Therefore, in other situations, where the quality or the amount of the medium would be different, the release profile could be different. For example, in the periodontal pocket, where only a slow flow of sulcus fluid exists, leaking of the drug could be substantially altered. In the literature we can find various drugs used in clinical practice that could be effective alone, or as a part

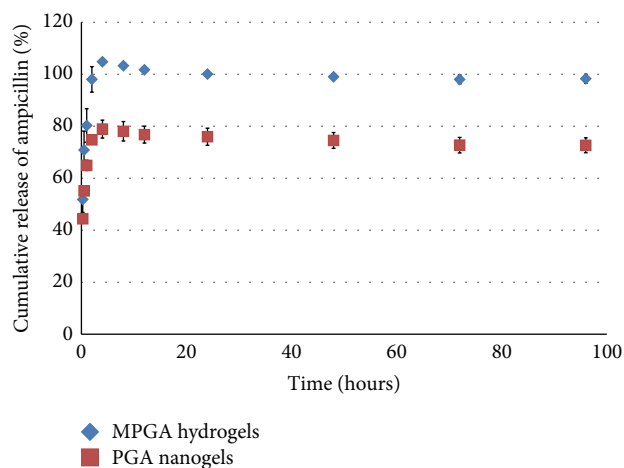


FIGURE 8: The ampicillin release properties of the hydrogel/nanogel systems.

of the treatment of periodontal diseases. The application of these drug delivery systems is well established [38]. They can be used in diverse ways according to the clinical situation. The application of drug solutions or ointments, or in other cases embedding drugs in crosslinked-polymer matrices or fibers, can help us change or control the release profiles of the active components. Jhinger et al. compare the effectiveness of two drug delivery systems, microbeads and standard crosslinked polymer matrix controlled release [39]. This microformulation of drugs is one of the newest ideas that we can find on the market. Nanosized drug delivery systems for periodontal treatment are not available yet, but there are some other areas where we already benefit from the application of nanotechnology [40]. Based on these ideas this *in vitro* study could be the first step towards a new drug delivery system, and this concept can give us a good candidate for a more effective treatment of periodontal diseases.

All of the measurements were performed in at least three parallel experiments for the purpose of statistical analysis, except for the mechanical testing ( $n = 10$ ), the swelling ( $n = 5$ ), and the microbiological experiments ( $n = 4$ ).

The effect of the antibiotic ampicillin in free form and loaded into nanogel was compared with a microbiological method (Figure S1 and Table S1 in Supplementary Material available online at <http://dx.doi.org/10.1155/2016/7350516>). Ampicillin released from the nanogel created a somewhat (90–95%) smaller plaque on an *E. coli* lawn compared to ampicillin solution. Based on these results we conclude that although ampicillin releases are similar, the nanogel still has a slight retaining effect.

### 3.3. Biocompatibility of the PGA Nanogel

**3.3.1. Alamar Blue Viability Test and Proliferation Imaging Methods.** Toxicity of the PGA nanogels was examined by Alamar Blue assay using human osteosarcoma cell line (SAOS-2). In this set of experiments nanogels were submerged in the growth medium used by Millicell hanging cell culture inserts. During Alamar Blue treatment, the

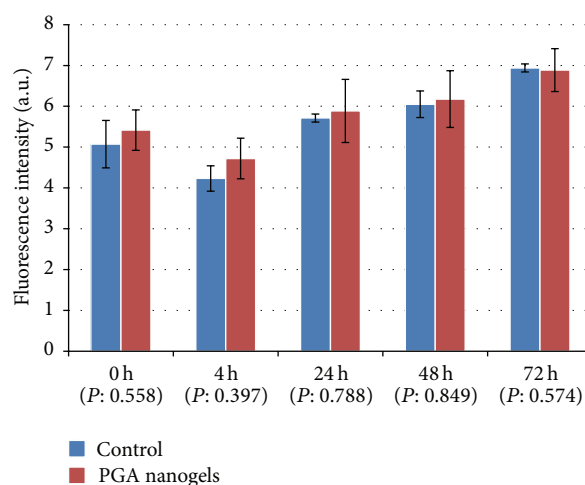


FIGURE 9: Alamar Blue assays for comparison of control and PGA nanogel-treated cells in self-control measurements. Mean fluorescence intensities were normalized to the weight of the nanogels.  $P$  values are in parentheses. Note: control group was 2D grown SAOS-2 cells without nanogel. Error bars represent the SD of three parallel measurements.

nanogels were removed and they were placed back after the measurement to continue the nanogel immersion. Thus a self-control analysis could be performed by measuring the same cells, keeping them alive for 72 hours, and changing the growth medium at every measurement. Three parallel measurements were performed to compare PGA nanogel-treated cells and untreated control cells. The results showed that no significant difference could be observed between the control and nanogel-treated cells.

According to the statistical analysis of the data at all time points, the mean values are the same on the basis of the  $t$ -tests. The  $P$  values of the appropriate  $t$ -tests can be seen in Figure 9 in parentheses. The Mann-Whitney test gave similar results; namely, the  $P$  values were far greater than 10% in all cases. The ANOVA with factors time (hours) and group (control and PGA nanogels) also gave the conclusion that the data did not show difference between the different groups ( $P$  value > 0.8), but they clearly showed significant difference in time.

Cell attachment to the nanogel surface is an important aspect of biocompatibility. As Figure 10 illustrates, living cells are attached to the PGA nanogel and to the coverslip in comparable amounts at the 6-hour time point (Figures 10(a) and 10(f)). Green Tracker staining shows living cells in green, while propidium iodide staining shows the nucleus of the dead cells in red. While cells proliferate evenly on the coverslip surface (Figures 10(a)–10(e)), they form clusters of different sizes on the hydrogel as it was demonstrated earlier on 3D scaffolds [41–43]. These clusters grow in size as SAOS-2 cells proliferate (Figures 10(f)–10(j)). The increasing size of the clusters and the very few observable dead cells support the result of the Alamar Blue test, namely, the fact that this PGA nanogel is cytocompatible.

Cell morphology on the hydrogel is similar to the natural spheroid phenotype, which is usual in 3D scaffolds, and these cells create clusters (Figures 10(f)–10(j)) [43]. This is



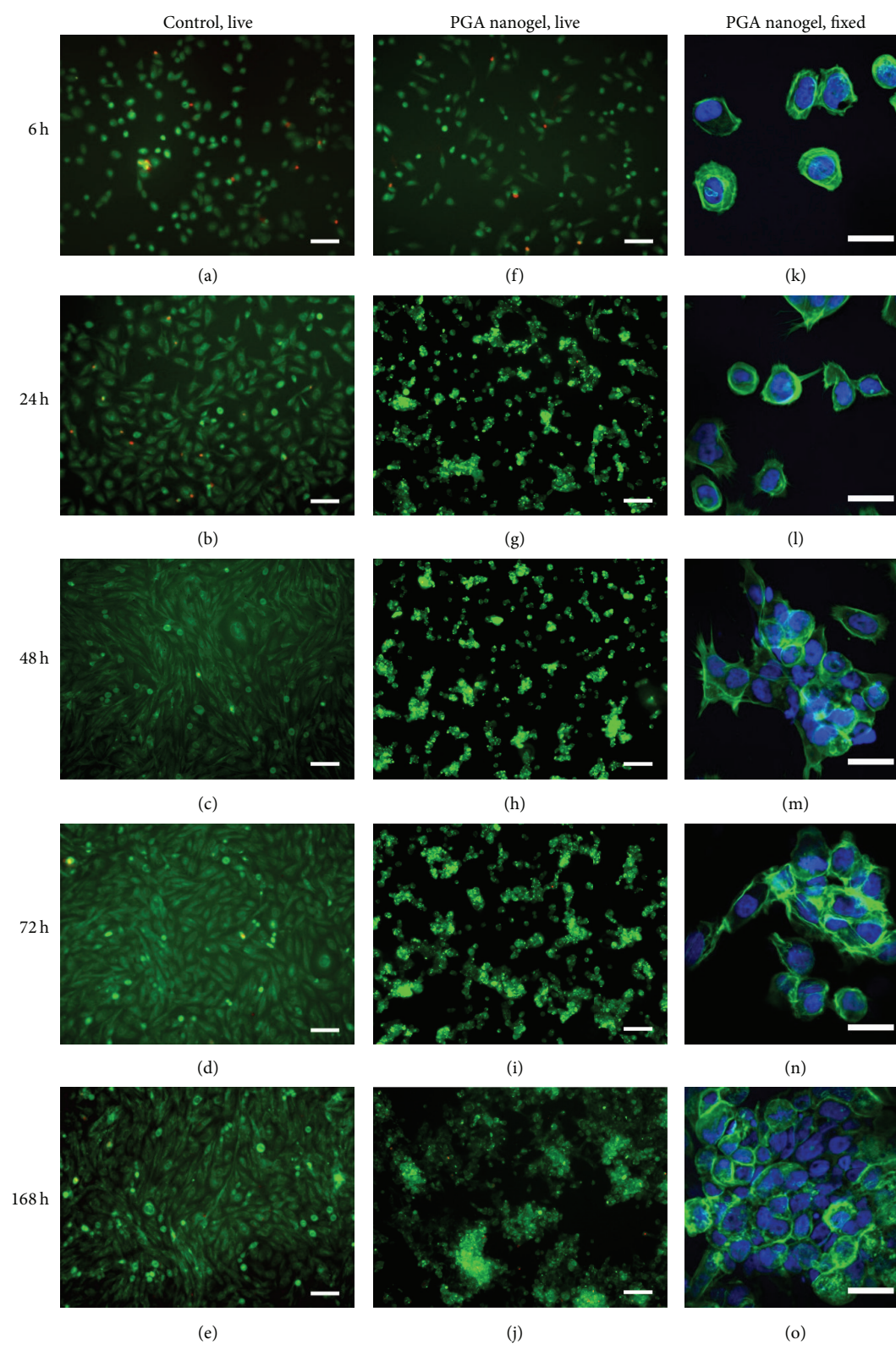


FIGURE 10: Fluorescence microscopy images of SAOS-2 cells on control (glass) surface (a)–(e) and on PGA nanogel hydrogels (f)–(j), and confocal laser scanning microscopy pictures from SAOS-2 cells on PGA nanogels (k)–(o). Notes: bars are 100  $\mu\text{m}$  on pictures (a)–(j) and 30  $\mu\text{m}$  on (k)–(o).



in contrast to the coverslip control, where the cells grow in 2D and show flat phenotype (Figures 10(a)–10(e)). This is the reason that in the case of flat surface the density of the cells is growing, while in the case of PGA nanogel the sizes of clusters are increased. When the cytoskeleton is stained with Alexa488 conjugated phalloidin, higher magnification with confocal imaging clearly shows the natural spherical morphology of the cells attached to the nanogel and represents the different structures of the clusters (Figures 10(k)–10(o)).

#### 4. Conclusion

In this study a visible (blue) light polymerizable hydrogel system was demonstrated, which was created solely from methacrylated-PGA nanoparticles. The reactive nanoparticles were characterized by DLS measurements and could be recognized in SEM images. The swelling and mechanical properties of the created PGA nanogel allow for the production of a suitable candidate for a system that can be used directly in the mouth. The release behavior provides control possibilities because the nanoparticle-created hydrogel (PGA nanogel) retains a part of the antibiotic drug. Biocompatibility of the nanogel was verified by Alamar Blue and confocal microscopy. The Alamar Blue test showed that the PGA nanogel would not cause any side effects, and the microscopy techniques proved the viability and morphology of the cells. The described properties and the possibility of *in situ* applications offer flexible drug dosage. The opportunity of direct administration means better therapeutic effect of different antibiotic drugs or any other bioactive factors.

#### Competing Interests

The authors declare that there is no conflict of interests regarding the publication of this paper.

#### Acknowledgments

This research was supported by the European Union and the State of Hungary and cofinanced by the European Social Fund in the framework of TÁMOP 4.2.4. A/2-11-1-2012-0001 “National Excellence Program” and research infrastructure by TAMOP-4.2.2.A-11/1/KONV-2012-0036 project.

#### References

- [1] A. K. Gaharwar, N. A. Peppas, and A. Khademhosseini, “Nanocomposite hydrogels for biomedical applications,” *Biotechnology and Bioengineering*, vol. 111, no. 3, pp. 441–453, 2014.
- [2] H. Nehoff, N. N. Parayath, L. Domanovitch, S. Taurin, and K. Greish, “Nanomedicine for drug targeting: strategies beyond the enhanced permeability and retention effect,” *International Journal of Nanomedicine*, vol. 9, no. 1, pp. 2539–2555, 2014.
- [3] E. A. A. Neel, L. Bozec, R. A. Perez, H.-W. Kim, and J. C. Knowles, “Nanotechnology in dentistry: prevention, diagnosis, and therapy,” *International Journal of Nanomedicine*, vol. 10, pp. 6371–6394, 2015.
- [4] W. Lohcharoenkal, L. Wang, Y. C. Chen, and Y. Rojanasakul, “Protein nanoparticles as drug delivery carriers for cancer therapy,” *BioMed Research International*, vol. 2014, Article ID 180549, 12 pages, 2014.
- [5] M. J. Choi, A. M. McDonagh, P. Maynard, and C. Roux, “Metal-containing nanoparticles and nano-structured particles in fingerprint detection,” *Forensic Science International*, vol. 179, no. 2–3, pp. 87–97, 2008.
- [6] J. Duan, J. Jiang, J. Li, L. Liu, Y. Li, and C. Guan, “The preparation of a highly stretchable cellulose nanowhisker nanocomposite hydrogel,” *Journal of Nanomaterials*, vol. 2015, Article ID 963436, 8 pages, 2015.
- [7] J. Mudassir, Y. Darwis, and P. K. Khiang, “Prerequisite characteristics of nanocarriers favoring oral insulin delivery: nanogels as an opportunity,” *International Journal of Polymeric Materials and Polymeric Biomaterials*, vol. 64, no. 3, pp. 155–167, 2015.
- [8] S. Mura, J. Nicolas, and P. Couvreur, “Stimuli-responsive nanocarriers for drug delivery,” *Nature Materials*, vol. 12, no. 11, pp. 991–1003, 2013.
- [9] M. Larsson, A. Bergstrand, L. Mesiah, C. Van Vooren, and A. Larsson, “Nanocomposites of polyacrylic acid nanogels and biodegradable polyhydroxybutyrate for bone regeneration and drug delivery,” *Journal of Nanomaterials*, vol. 2014, Article ID 371307, 9 pages, 2014.
- [10] H. B. Patel, H. L. Patel, Z. H. Shah, and M. K. Modasiya, “Review on hydrogel nanoparticles in drug delivery,” *American Journal of PharmTech Research*, vol. 1, no. 3, pp. 19–38, 2011.
- [11] B. V. N. Namburi, H. K. S. Yadav, S. Hemanth, A. Ahmed, V. L. Sureddy, and H. G. Shivakumar, “Formulation and evaluation of polymeric nanoparticulate gel for topical delivery,” *International Journal of Polymeric Materials and Polymeric Biomaterials*, vol. 63, no. 9, pp. 439–447, 2014.
- [12] K. Prasad, G. Vijay, N. K. Jayakumari, A. Dhananjaya, and L. Valliyil, “Nanogel as a smart vehicle for local drug delivery in dentistry,” *American Journal of Pharmacy and Health Research*, vol. 3, no. 1, pp. 19–30, 2015.
- [13] A. H. Doulabi, H. Mirzadeh, N. Samadi, S. Bagheri-Khoulenjani, M. Atai, and M. Imani, “Potential application of a visible light-induced photocured hydrogel film as a wound dressing material,” *Journal of Polymers*, vol. 2015, Article ID 867928, 10 pages, 2015.
- [14] Q. Zia, A. A. Khan, Z. Swaleha, and M. Owais, “Self-assembled amphotericin B-loaded polyglutamic acid nanoparticles: preparation, characterization and in vitro potential against *Candida albicans*,” *International Journal of Nanomedicine*, vol. 10, pp. 1609–1623, 2015.
- [15] S. J. Buwalda, K. W. M. Boere, P. J. Dijkstra, J. Feijen, T. Vermonden, and W. E. Hennink, “Hydrogels in a historical perspective: from simple networks to smart materials,” *Journal of Controlled Release*, vol. 190, pp. 254–273, 2014.
- [16] R. Censi, P. Di Martino, T. Vermonden, and W. E. Hennink, “Hydrogels for protein delivery in tissue engineering,” *Journal of Controlled Release*, vol. 161, no. 2, pp. 680–692, 2012.
- [17] X. Wang, T. Hao, J. Qu, C. Wang, and H. Chen, “Synthesis of thermal polymerizable alginate-GMA hydrogel for cell encapsulation,” *Journal of Nanomaterials*, vol. 2015, Article ID 970619, 8 pages, 2015.
- [18] F. Alexis, E. Pridgen, L. K. Molnar, and O. C. Farokhzad, “Factors affecting the clearance and biodistribution of polymeric nanoparticles,” *Molecular Pharmaceutics*, vol. 5, no. 4, pp. 505–515, 2008.
- [19] M. Siyawamwaya, Y. E. Choonara, D. Bijukumar, P. Kumar, L. C. Du Toit, and V. Pillay, “A review: overview of novel

- polyelectrolyte complexes as prospective drug bioavailability enhancers,” *International Journal of Polymeric Materials and Polymeric Biomaterials*, vol. 64, no. 18, pp. 955–968, 2015.
- [20] S. R. Hwang and K. Kim, “Nano-enabled delivery systems across the blood-brain barrier,” *Archives of Pharmacal Research*, vol. 37, no. 1, pp. 24–30, 2014.
- [21] I. Bajaj and R. Singhal, “Poly (glutamic acid)—an emerging biopolymer of commercial interest,” *Bioresource Technology*, vol. 102, no. 10, pp. 5551–5561, 2011.
- [22] A. Ogunleye, A. Bhat, V. U. Irorere, D. Hill, C. Williams, and I. Radecka, “Poly- $\gamma$ -glutamic acid: production, properties and applications,” *Microbiology*, vol. 161, no. 1, pp. 1–17, 2015.
- [23] W. Zeng, W.-K. Hu, H. Li et al., “Preparation and characterization of Poly( $\gamma$ -glutamic acid) hydrogels as potential tissue engineering scaffolds,” *Chinese Journal of Polymer Science*, vol. 32, no. 11, pp. 1507–1514, 2014.
- [24] W. P. Chan, F.-C. Kung, Y.-L. Kuo, M.-C. Yang, and W.-F. T. Lai, “Alginate/poly( $\gamma$ -glutamic acid) base biocompatible gel for bone tissue engineering,” *BioMed Research International*, vol. 2015, Article ID 185841, 7 pages, 2015.
- [25] J. Bako, M. Szepesi, A. J. Veres et al., “Synthesis of biocompatible nanocomposite hydrogels as a local drug delivery system,” *Colloid and Polymer Science*, vol. 286, no. 3, pp. 357–363, 2008.
- [26] T. Akagi, F. Shima, and M. Akashi, “Intracellular degradation and distribution of protein-encapsulated amphiphilic poly(amino acid) nanoparticles,” *Biomaterials*, vol. 32, no. 21, pp. 4959–4967, 2011.
- [27] F. Shima, T. Akagi, T. Uto, and M. Akashi, “Manipulating the antigen-specific immune response by the hydrophobicity of amphiphilic poly( $\gamma$ -glutamic acid) nanoparticles,” *Biomaterials*, vol. 34, no. 37, pp. 9709–9716, 2013.
- [28] R. Toita, K. Nakao, A. Mahara, T. Yamaoka, and M. Akashi, “Biodistribution of vaccines comprised of hydrophobically-modified poly( $\gamma$ -glutamic acid) nanoparticles and antigen proteins using fluorescence imaging,” *Bioorganic and Medicinal Chemistry*, vol. 21, no. 21, pp. 6608–6615, 2013.
- [29] J. Bakó, M. Vecsernyés, Z. Ujhelyi et al., “Composition and characterization of in situ usable light cured dental drug delivery hydrogel system,” *Journal of Materials Science: Materials in Medicine*, vol. 24, no. 3, pp. 659–666, 2013.
- [30] J. É. F. Radu, L. Novak, J. F. Hartmann et al., “Structural and dynamical characterization of poly-gamma-glutamic acid-based cross-linked nanoparticles,” *Colloid and Polymer Science*, vol. 286, no. 4, pp. 365–376, 2008.
- [31] M. Petrás, T. Lajtos, E. Friedländer et al., “Molecular interactions of ErbB1 (EGFR) and integrin- $\beta$ 1 in astrocytoma frozen sections predict clinical outcome and correlate with Akt-mediated in vitro radioresistance,” *Neuro-Oncology*, vol. 15, no. 8, pp. 1027–1040, 2013.
- [32] G. Tronci, C. A. Grant, N. H. Thomson, S. J. Russell, and D. J. Wood, “Multi-scale mechanical characterization of highly swollen photo-activated collagen hydrogels,” *Journal of the Royal Society Interface*, vol. 12, no. 102, Article ID 20141079, 2015.
- [33] J. S. Colombo, A. N. Moore, J. D. Hartgerink, and R. N. D’Souza, “Scaffolds to control inflammation and facilitate dental pulp regeneration,” *Journal of Endodontics*, vol. 40, no. 4, pp. S6–S12, 2014.
- [34] F. T. Moutos and F. Guilak, “Functional properties of cell-seeded three-dimensionally woven poly( $\epsilon$ -Caprolactone) scaffolds for cartilage tissue engineering,” *Tissue Engineering A*, vol. 16, no. 4, pp. 1291–1301, 2010.
- [35] T. Garg and A. K. Goyal, “Biomaterial-based scaffolds—current status and future directions,” *Expert Opinion on Drug Delivery*, vol. 11, no. 5, pp. 767–789, 2014.
- [36] I. D. Gaudet and D. I. Shreiber, “Characterization of methacrylated type-I collagen as a dynamic, photoactive hydrogel,” *Biointerphases*, vol. 7, no. 1–4, p. 25, 2012.
- [37] L. Shi, N. Yang, H. Zhang et al., “A novel poly( $\gamma$ -glutamic acid)/silk-sericin hydrogel for wound dressing: synthesis, characterization and biological evaluation,” *Materials Science and Engineering C*, vol. 48, pp. 533–540, 2015.
- [38] H. A. Da Rocha, C. F. Silva, F. L. Santiago, L. G. Martins, P. C. Dias, and D. De, “Local drug delivery systems in the treatment of periodontitis: a literature review,” *International Academy of Periodontology*, vol. 17, no. 3, pp. 82–90, 2015.
- [39] N. Jhinger, D. Kapoor, and R. Jain, “Comparison of Periochip (chlorhexidine gluconate 2.5 mg) and Arestin (Minocycline hydrochloride 1 mg) in the management of chronic periodontitis,” *Indian Journal of Dentistry*, vol. 6, no. 1, pp. 20–26, 2015.
- [40] R. S. Narang and J. K. Narang, “Nanomedicines for dental applications—scope and future perspective,” *International Journal of Pharmaceutical Investigation*, vol. 5, no. 3, pp. 121–123, 2015.
- [41] W. E. G. Müller, H. C. Schröder, Q. Feng, U. Schlossmacher, T. Link, and X. Wang, “Development of a morphogenetically active scaffold for three-dimensional growth of bone cells: Biosilica-alginate hydrogel for SaOS-2 cell cultivation,” *Journal of Tissue Engineering and Regenerative Medicine*, vol. 9, no. 11, pp. E39–E50, 2015.
- [42] E. S. Place, L. Rojo, E. Gentleman, J. P. Sardinha, and M. M. Stevens, “Strontium-and zinc-alginate hydrogels for bone tissue engineering,” *Tissue Engineering A*, vol. 17, no. 21–22, pp. 2713–2722, 2011.
- [43] C. Trojani, P. Weiss, J.-F. Michiels et al., “Three-dimensional culture and differentiation of human osteogenic cells in an injectable hydroxypropylmethylcellulose hydrogel,” *Biomaterials*, vol. 26, no. 27, pp. 5509–5517, 2005.



